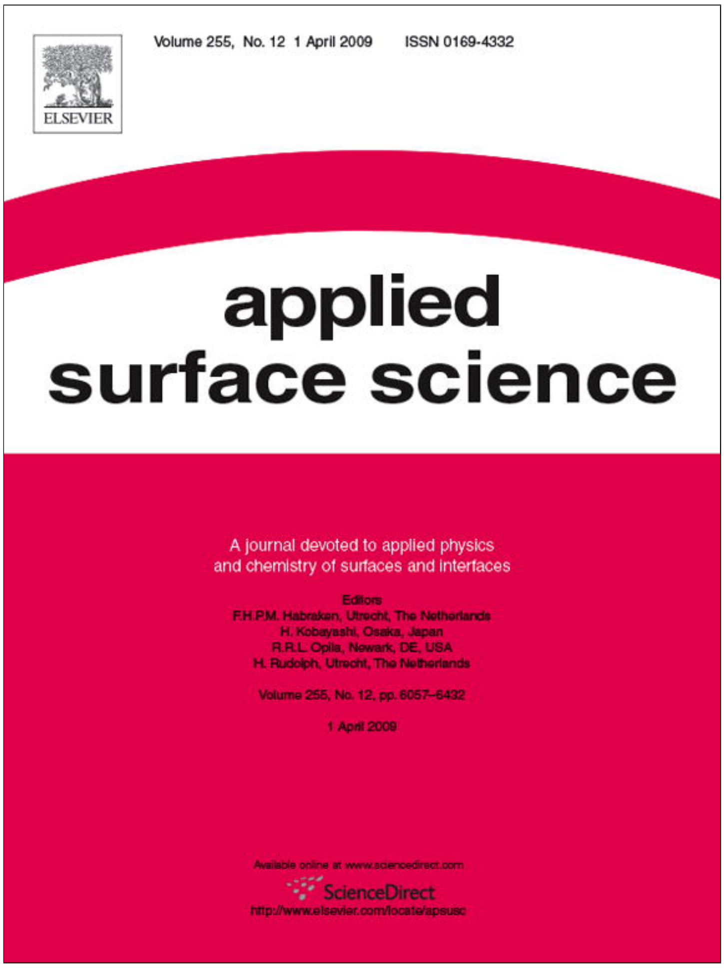
Volume 255, No. 12 1 April 2009 ISSN 0169-4332
ELSEVIER
applied
surface science
A journal devoted to applied physics
and chemistry of surfaces and interfaces
Editors
F.H.P.M. Habraken, Utrecht, The Netherlands
H. Kobayashi, Osaka, Japan
R.R.L. Opila, Newark, DE, USA
H. Rudolph, Utrecht, The Netherlands
Volume 255, No. 12, pp. 6057–6432
1 April 2009
Available online at www.sciencedirect.com
ScienceDirect
http://www.elsevier.com/locate/apsusc

Applied Surface Science 255 (2009) 6262–6265

Contents lists available at ScienceDirect

Applied Surface Science

journal homepage: www.elsevier.com/locate/apsusc

Numerical analysis of the transport processes in manganite–titanate Schottky junctions

Peng Han [a,b,*], Jin-Feng Jia [a], Meng He [b]

[a] Department of Physics, Tsinghua University, Haidian District, Beijing 100084, China
[b] Institute of Physics, Chinese Academy of Sciences, Beijing 100190, China

ARTICLE INFO

Article history:
Received 1 September 2008
Accepted 31 January 2009
Available online 10 February 2009

PACS:
73.40.Lq
77.84.Dy
72.20.−i

Keywords:
Perovskite oxide
Schottky junction
Transport

ABSTRACT

A numerical study is presented on the transport processes in the manganite–titanate Schottky junction by using the Poisson equation, the drift-diffusion formulas, the direct and thermally assisted tunneling model. Comparing with the experimental data, it is found that the non-monotonically temperature-dependent *I–V* curves under reverse bias is caused by the competition between the direct and thermally assisted tunneling processes. In addition, it is also found that the electric field dependence of the permittivity in Nb-doped $SrTiO_3$ plays an important role on the transport properties of the manganite–titanate Schottky junctions based on our calculation.

1. Introduction

The Nb-doped $SrTiO_3$ (SNTO) is one of the most intensively studied oxide material because of its intriguing properties such as the high dielectric constant [1], the strongly electric field dependent permittivity [2,3], the small in-plane lattice mismatch with perovskite oxides [4,5], and the complicated interface states [6]. Recently, the SNTO-based p–n junctions [7–11], field effect transistors [12], multilayer structures [13], and Schottky junctions [2,5,6,14–16] have been fabricated by many groups. Among them, the SNTO-based Schottky junctions have attracted much attention not only because they are ideal platforms to probe the complicated interface states of SNTO in the field of fundamental research [2] but also they are good candidates for the spintronic devices [6] and non-volatile memory cells [16] in the real application. Although the vigorous experimental efforts [2,5,6,15,16] have been carried out in the SNTO-based Schottky junctions, a self-consistent description of the transport processes in these junctions is still lacking. In addition, the physical origins for the magnetoresistance (MR) effect [2] and the electroresistance (ER) effect [15] observed in the SNTO-based Schottky junctions are unclear. Thus, a theoretical study on the transport processes in the Schottky junctions of manganite–titanate is urgently to be given.

Recently, a phenomenological model based on Poisson equation, the drift-diffusion model and the continuity equations has been proposed [8,17,18] to analyze the transport mechanisms in the multi-correlated perovskite oxide p–n junctions. With this model, the transport processes in the all-oxide [17–19] and oxide-silicon [20,21] p–n junctions have been well explained with both forward and reverse bias voltages. This provides the possibility to give a self-consistent analysis on the transport properties of the perovskite oxide Schottky junctions.

In this paper, a numerical study on the transport processes in the Schottky junction of $La_{0.7}Sr_{0.3}MnO_3$/Nb:$SrTiO_3$ (LSMO/SNTO) is given with taking into account the strongly electric field dependent permittivity of SNTO at both forward and reverse bias. The comparison between the calculated and the measured *I–V* curves reveals that the non-monotonically temperature-dependent current observed at reverse bias is induced by the competition between the direct and the thermally assisted tunneling processes. It is also found that the strongly electronic field dependence of permittivity in SNTO plays a very important role on the transport properties in the LSMO/SNTO Schottky junction with forward bias. In addition, a novel bias voltage dependent resistance of LSMO/SNTO Schottky junction is found based on our calculation.

2. Theoretical model

The distributions of electrostatic potential $\phi(x)$, electrons $n(x)$, holes $p(x)$ in the LSMO/SNTO Schottky junction under external bias

* Corresponding author at: Department of Physics, Tsinghua University, Haidian District, Beijing 100084, China. Tel.: +86 10 82649176; fax: +86 10 82649176.
E-mail address: hanpeng@aphy.iphy.ac.cn (P. Han).

0169-4332/$ – see front matter © 2009 Elsevier B.V. All rights reserved.
doi:10.1016/j.apsusc.2009.01.095

voltage V_{bias} are calculated by solving Poisson equation, the drift-diffusion formulas, and the continuity equations self-consistently with the Richardson thermionic emission current as the interface condition [22–24]. Considering the electric field and temperature dependence of permittivity $\varepsilon_r(\mathcal{E}(x), T)$ in the SNTO material, Poisson equation is expressed as

$$-\frac{d^2\phi(x)}{dx^2} = \frac{q}{\varepsilon_0\varepsilon_r(\mathcal{E}(x), T)}[p(x) - n(x) + N_d], \tag{1}$$

where q denotes the electron charge, ε_0 is the dielectric constant of vacuum, and N_d represents the ionized donor density of SNTO, respectively. The electric field dependence of permittivity is approximated by $\varepsilon_r(\mathcal{E}(x), T) = b(T)/\sqrt{a(T) + \mathcal{E}^2(x)}$ with the parameters $a(T) = [(\coth(44.1/T) - 0.937)/1635]b(T)$, $b(T) = 1.39\times 10^7 + 4.29 \times 10^5 T$ V/cm [25,26], and the electric field intensity $\mathcal{E}(x) = -d\phi(x)/dx$, respectively. The drift-diffusion and continuity equations, the boundary conditions, and the detailed arithmetic for solving these formulas have been given in elsewhere [17,22,23]. Based on the calculation, the band-energy profile of the LSMO/SNTO Schottky junction under reverse bias is given in Fig. 1. As shown in this figure, the tunneling process is divided into two parts. When a forward bias voltage is applied to the Schottky junction, the tunneling process with electrons between the bottom of the conduction band E_c and the Fermi level E_{fn} for semiconductor is defined as the direct tunneling. In another process, electrons are first thermally excited to an energy between E_{fn} and the top of the barrier E_{top} and then tunnel into the metallic LSMO. And this process is defined as thermally assisted tunneling. For the reverse-biased Schottky junction, the electrons with energy between E_c and the Fermi level for metal E_{fM} and the thermally exited electrons with energy between E_{fM} and E_{top} can tunnel into the n-SNTO region directly and indirectly, respectively.

With taking into account the direct and thermally assisted tunneling processes, the currents with forward and reverse bias J_F and J_R are expressed as

$$J_F = A^*T^2\exp\left(-\frac{q\Phi_B}{k_BT}\right)\left[\exp\left(\frac{qV_{bias}}{k_BT}\right) - 1\right] + q\int_{E_c}^{E_{top}} \frac{N(E)T(E)}{1+\exp\left(\frac{E-E_{fn}}{k_BT}\right)}dE \tag{2}$$

and

$$J_R = A^*T^2\exp\left(-\frac{q\Phi_B}{k_BT}\right)\left[\exp\left(\frac{qV_{bias}}{k_BT}\right) - 1\right] - q\int_{E_c}^{E_{top}} \frac{N(E)T(E)}{1+\exp\left(\frac{E-E_{fM}}{k_BT}\right)}dE, \tag{3}$$

where A^* is the effective Richardson constants of electron, Φ_B represents the effective barrier height of the Schottky junction, $N(E)$ is the density of states, and k_B denotes Boltzmann's constant, respectively. The tunneling rate $T(E) = (\hbar/\sqrt{2m_c^*E})\Im[\psi_E^*(x)(d/dx)\psi_E(x)]$ with "$\Im$" denotes the imaginary part of a complex number, $\hbar$ is the reduced Planck constant, and m_c^* denotes the electron effective mass, respectively. The wave function $\psi_E(x)$ is solved by using the free electron approximation and the finite-difference schemes [19,27].

3. Results and discussion

With these formulas, the I–V characteristics of a LSMO/SNTO Schottky junction with $N_d = 3.0 \times 10^{20}$ cm^{-3} are calculated self-consistently at T = 100, 200, 300, and 400 K, respectively. In the calculation, the Schottky barrier height is taken as 1.2 eV [6], the effective mass of electrons for SNTO is $1.3m_0$ with m_0 being the mass for free electron [28], and the other necessary parameters are taken from Ref. [17] and [18], respectively. The calculated I–V curves with applied bias voltages from negative to positive are given in Fig. 2, while the detailed I–V characteristics under reverse bias are plotted in the inset. Comparing our theoretical results with the experimental data reported in Ref. [16], it is found that the thermoionic emission current, the direct and thermally assisted tunneling currents dominate the forward transport process in the LSMO/SNTO Schottky junction, while the direct and thermally assisted tunneling processes are the mainly transport mechanisms at reverse bias. To reveal the physical origin of the non-monotonically temperature-dependent I–V curves observed at reverse bias [16], we plot the direct tunneling current (dashed curve), the thermally assisted tunneling current (dotted curve) and the total tunneling current (solid curves) with T = 100, 300, and 400 K in Fig. 3(a), (b), and (c), respectively. As indicated in these figures, the density of direct tunneling current decreases and that

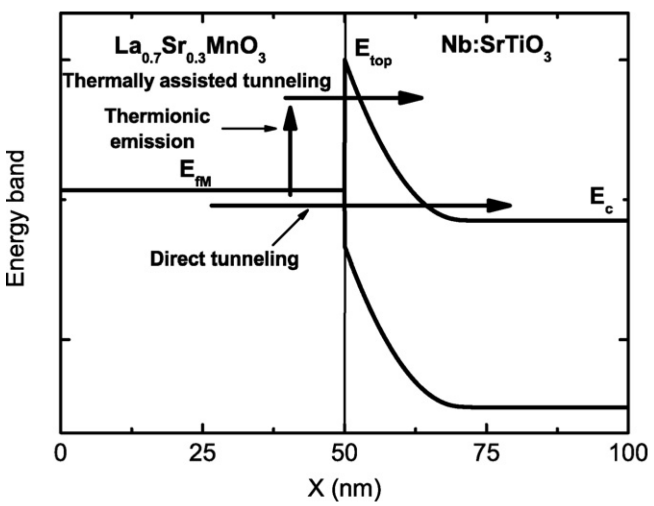

Fig. 1. The band energy of the $La_{0.7}Sr_{0.3}MnO_3$/Nb:$SrTiO_3$ Schottky junction with reverse bias at T = 300 K with concentration of donor N_d as 3.0×10^{19} cm^{-3}.

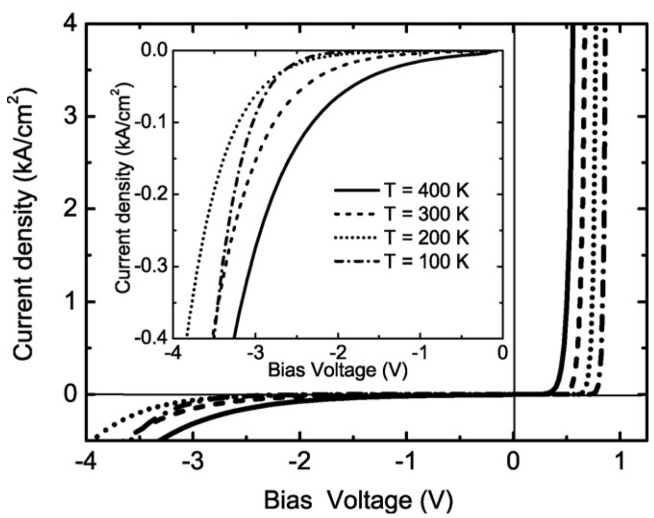

Fig. 2. The theoretical I–V characteristics with applied bias voltage from negative to positive at T = 100 K (dashed and dotted curve), 200 K (dotted curve), 300 K (dashed curve), and 400 K (solid curves), respectively. The inset shows the I–V curves under reverse bias at various temperatures.

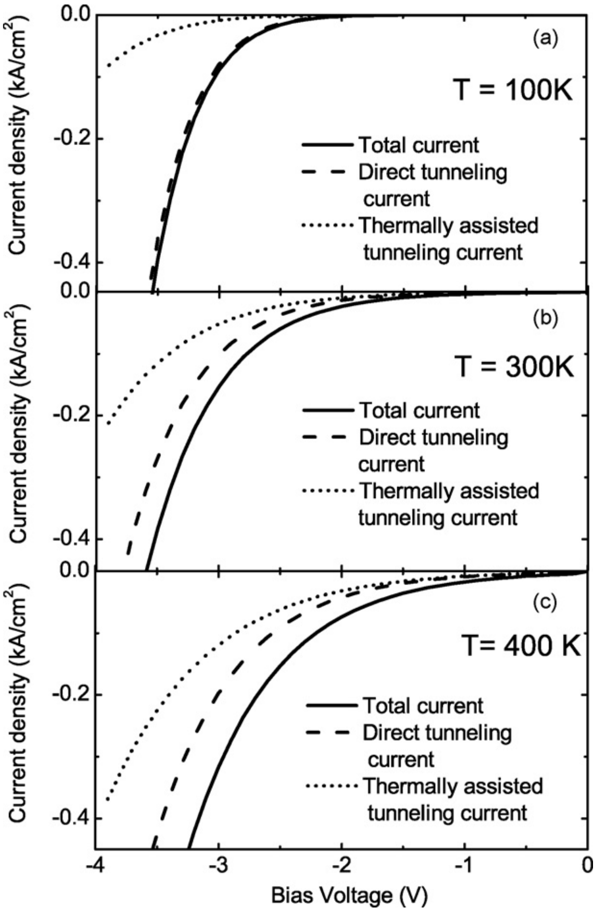

Fig. 3. The comparison between the direct tunneling current, the thermally assisted tunneling current, and the total tunneling current under applied reverse bias voltages at $T = 100$ K (a), 300 K (b), and 400 K (c), respectively.

of thermally assisted tunneling current increases with the increase of temperature. Thus, the non-monotonically temperature-dependent current observed at reverse bias is attributed to the competition between the direct and the thermally assisted tunneling processes.

For the further study on the transport properties of SNTO-based Schottky junction, we plot the value of $\Delta R/R = [R(V_{bias}) - R(0.01\,\text{V})]/R(0.01\,\text{V})$ with $T = 100$, 120, 140, 160, and 200 K at forward and reverse bias in Fig. 4(a) and (b), respectively. As shown in Fig. 4(a), the value of $\Delta R/R$ increases with the increased forward bias and obtains its peak value at a certain bias voltage, and then decreases with the further increase of the bias. In addition, it is also found that the value of $\Delta R/R$ decreases with the increased temperature at a certain applied bias voltage. In Fig. 4(b), the value of $\Delta R/R$ decreases with the increased reverse bias monotonically at a certain temperature and decreases with the decreased temperature under a certain applied bias voltage, respectively. These intriguing behaviors can be explained as follows. When a forward bias voltage is applied to the Schottky junction, the intensity of electric field in the space charge region decreases and the electric field dependent permittivity increases, thereby increasing the width of the Schottky barrier. The electric field dependent permittivity in the SNTO region of LSMO/SNTO Schottky junction under both forward and reverse bias at $T = 100$ and 200 K is plotted in Fig. 5(a) and (b), respectively. On the other hand, the thermoionic emission current increases exponentially with the increased forward bias according to Eq. (2). The competition between the increased barrier width and the thermoionic emission current induces a peak value of $\Delta R/R$ at a certain forward bias. As

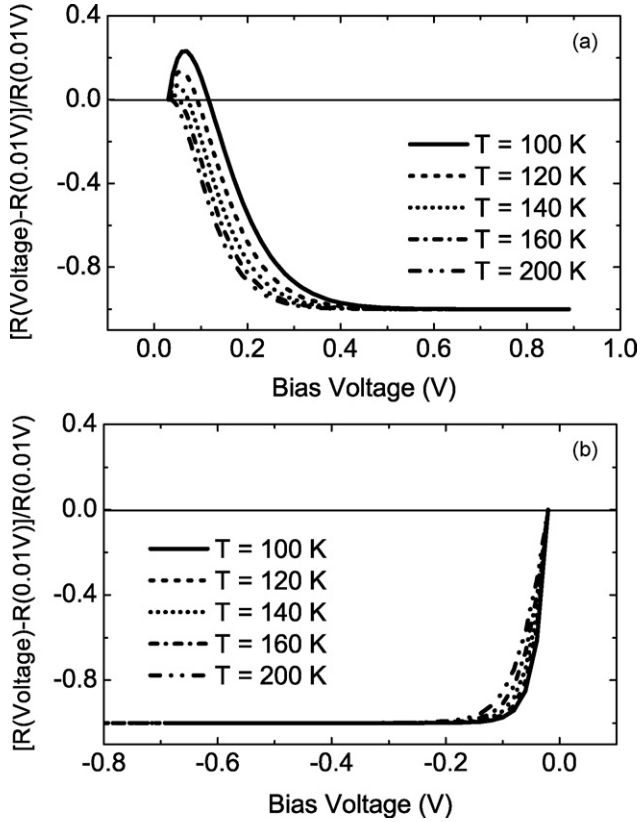

Fig. 4. The calculated $\Delta R/R = [R(V_{bias}) - R(0.01\,\text{V})]/R(0.01\,\text{V})$ with forward (a) and reverse bias (b) at various temperatures.

indicated in Fig. 5(a) and (b), the electric field dependent permittivity decreases with the increased temperature, thereby reducing the width of Schottky barrier. In addition to the decrease of barrier width, the rapidly increased thermoionic emission

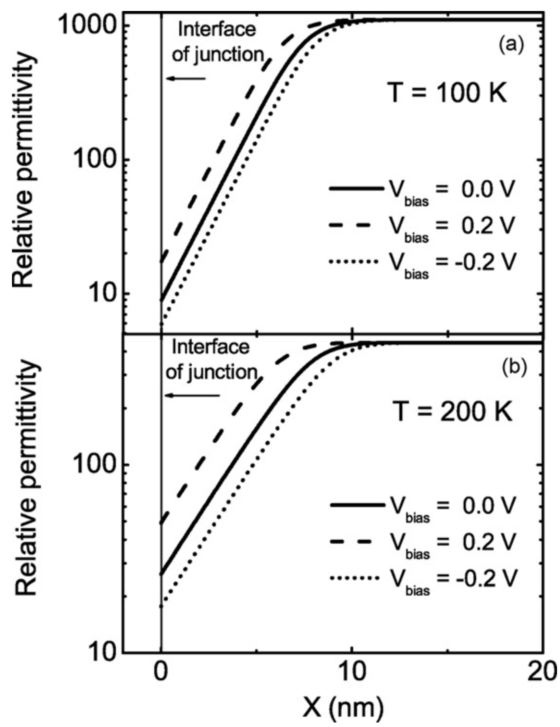

Fig. 5. The electric field dependence of relative permittivity with $V_{bias} = 0.0$ V (solid curve), 0.2 V (dashed curve), and -0.2 V (dotted curve) at $T = 100$ K (a) and 200 K (b), respectively.

current dominates the transport process and reduces the value of $\Delta R/R$ with the increase of temperature. In the case of reverse bias, the width of the Schottky barrier decreases and there are more available unoccupied states on the n-SNTO side with the increase of bias voltage. And these result in the increase of current and the monotonic decrease of $\Delta R/R$ with the increased reverse bias.

4. Summary

In summary, the transport processes in LSMO/SNTO Schottky junction have been studied self-consistently with taking into account the electric field dependent permittivity of SNTO material. Comparing with the calculated results and the experimental data, it is found that the thermoionic emission current, the direct and thermally assisted tunneling currents are the mainly transport mechanisms in the LSMO/SNTO Schottky junction, and the non-monotonically temperature-dependent I–V characteristics is induced by the competition between the direct and the thermally assisted tunneling current. Based on our calculation, it is also found that the value of $\Delta R/R = [R(V_{bias}) - R(0.01\,\mathrm{V})]/R(0.01\,\mathrm{V})$ exhibits a novel property with the increased forward bias, and this behavior is attributed to the electric field dependence of permittivity in the SNTO material.

Acknowledgements

P.H. acknowledges Prof. K. -j. Jin for her helpful discussions. This work was supported by the National Natural Science Foundation of China, and the National Basic Research Program of China.

References

[1] K.A. Müller, H. Burkard, Phys. Rev. B 19 (1979) 3595.
[2] T. Susaki, Y. Kozuka, Y. Tateyama, H.Y. Hwang, Phys. Rev. B 76 (2007) 155110.
[3] T. Yamamoto, S. Suzuki, K. Kawaguchi, K. Takahashi, Jpn. J. Appl. Phys., Part 1 37 (1998) 4737.
[4] A. Vigliante, U. Gebhardt, A. Rühm, P. Wochner, F.S. Razavi, H.U. Habermeier, Europhys. Lett. 54 (2001) 619.
[5] T. Susaki, N. Nakagawa, H.Y. Hwang, Phys. Rev. B 75 (2007) 104409.
[6] M. Minohara, I. Ohkubo, H. Kumigashira, M. Oshima, Appl. Phys. Lett. 90 (2007) 132123.
[7] H.B. Lu, S.Y. Dai, Z.H. Chen, Y.L. Zhou, B.L. Cheng, K.J. Jin, L.F. Liu, G.Z. Yang, X.L. Ma, Appl. Phys. Lett. 86 (2005) 032502.
[8] K.-j. Jin, H.B. Lu, Q.L. Zhou, K. Zhao, B.L. Cheng, Z.H. Chen, Y.L. Zhou, G.Z. Yang, Phys. Rev. B 71 (2005) 184428.
[9] K. Zhao, Y.H. Huang, Q.L. Zhou, K.J. Jin, H.B. Lu, M. He, B.L. Cheng, Y.L. Zhou, Z.H. Chen, G.Z. Yang, Appl. Phys. Lett. 86 (2005) 221917.
[10] K.-j. Jin, K. Zhao, H.B. Lu, L. Liao, G.Z. Yang, Appl. phys. Lett. 91 (2007) 081906.
[11] H. Yang, H.M. Luo, H. Wang, I.O. Usov, N.A. Suvorova, M. Jain, D.M. Feldmann, P.C. Dowden, R.F. DePaula, Q.X. Jia, Appl. Phys. Lett. 92 (2008) 102113.
[12] H. Nakamura, H. Takagi, I.H. Inoue, Y. Takahashi, T. Hasegawa, Y. Tokura, Appl. Phys. Lett. 89 (2006) 133504.
[13] H.B. Lu, G.Z. Yang, Z.H. Chen, S.Y. Dai, Y.L. Zhou, K.J. Jin, B.L. Cheng, M. He, L.F. Liu, H.Z. Guo, Y.Y. Fei, W.F. Xiang, L. Yan, Appl. Phys. Lett. 84 (2004) 5007.
[14] T. Fujii, M. Kawasaki, A. Sawa, H. Akoh, Y. Kawazoe, Y. Tokura, Appl. Phys. Lett. 86 (2005) 012107.
[15] T. Fujii, M. Kawasaki, A. Sawa, Y. Kawazoe, H. Akoh, Y. Tokura, Phys. Rev. B 75 (2007) 165101.
[16] A. Ruotolo, C.Y. Lam, W.F. Cheng, K.H. Wong, C.W. Leung, Phys. Rev. B 76 (2007) 075122.
[17] Q.L. Zhou, K.J. Jin, H.B. Lu, P. Han, Z.H. Chen, K. Zhao, Y.L. Zhou, G.Z. Yang, Europhys. Lett. 71 (2005) 283.
[18] P. Han, K.J. Jin, H.B. Lu, Q.L. Zhou, Y.L. Zhou, G.Z. Yang, Appl. Phys. Lett. 91 (2007) 182102.
[19] P. Han, J.F. Jia, Phys. Lett. A 372 (2008) 4943.
[20] J. Qiu, K.J. Jin, P. Han, H.B. Lu, C.L. Hu, B.P. Wang, G.Z. Yang, Europhys. Lett. 79 (2007) 57004.
[21] C.L. Hu, P. Han, K.J. Jin, H.B. Lu, G.Z. Yang, J. Appl. Phys. 103 (2008) 053701.
[22] S.F. Guo, Solid-State Electron 27 (1984) 537.
[23] R.B. Darling, Solid-State Electron 31 (1988) 1031.
[24] J. Racko, D. Donoval, M. Barus, V. Nagl, A. Grmanova, Solid-State Electron 35 (1992) 913.
[25] S. Suzuki, T. Yamamoto, H. Suzuki, K. Kawaguchi, K. Takahashi, Y. Yoshisato, J. Appl. Phys. 81 (1997) 6830.
[26] J.H. Barrett, Phys. Rev. 86 (1952) 118.
[27] O. Pinaud, J. Appl. Phys. 92 (2002) 1987.
[28] T. Shimizu, H. Okushi, J. Appl. Phys. 85 (1999) 7244.